

Neurons Detect Increases and Decreases in Oxygen Levels Using Distinct Guanylate Cyclases

Manuel Zimmer, Jesse M. Gray, Navin Pokala, Andy J. Chang, David S. Karow, Michael A. Marletta, Martin L. Hudson, David B. Morton, Nikos Chronis, and Cornelia I. Bargmann

Supplementary materials

1. Strains
2. Molecular analysis of *gcy-31* and *gcy-33*
3. Plasmids for expression studies and transgenic rescue
4. Supplementary references
5. Supplementary table
6. Supplementary figures and legends

1. Strains

All strains were maintained under standard conditions (Brenner, 1974). Wild type was *C. elegans* Bristol strain N2. Other strains used in this study are: **RB564** *gcy-31(ok296)* X, **CX6448** *gcy-35(ok769)* I, **AX1297** *gcy-36(db66)* X, **CZ3715** *gcy-33(ok232)* V, **FK103** *tax-4(ks28)* III, **CX10131** *gcy-35(ok769)* I; *gcy-31(ok296)* X, **CX6803** *gcy-35(ok769)* I; *gcy-33(ok232)* V; *gcy-31(ok296)* X, **CX9553** *gcy-31(ok296)* X; *kyEx2028* [*WRM0630cF03 odr-1::DsRed2*], **CX9552** *gcy-31(ok296)* X; *kyEx2027* [*WRM0630cF03 odr-1::DsRed2*], **CX9684** *gcy-31(ok296)* X; *kyEx2117* [*gcy-31(genomic)::SL2::GFP odr-1::DsRed2*], **CX9683** *gcy-31(ok296)* X; *kyEx2116* [*gcy-31(genomic)::SL2::GFP odr-1::DsRed2*], **CX9620** *gcy-33(ok232)* V; *kyEx2086* [*gcy-31::gcy-33 odr-1::DsRed2*], **CX9618** *gcy-33(ok232)* V; *kyEx2084* [*gcy-31::gcy-33 odr-1::DsRed2*], **CX9560** *gcy-35(ok769)* I; *kyEx2033* [*gcy-35::gcy-35 odr-1::DsRed2*], **CX9565** *gcy-35(ok769)* I; *kyEx2038* [*gcy-35::gcy-35 odr-1::DsRed2*], **CX9563** *gcy-35(ok769)* I; *kyEx2036* [*flp-8::gcy-35 odr-1::DsRed2*], **CX9564** *gcy-35(ok769)* I; *kyEx2037* [*flp-8::gcy-35 odr-*

1::DsRed2], **CX9622** *gcy-36(db66)* X; *kyEx2088* [*gcy-36::gcy-36 odr-1::DsRed2*], **CX9621** *gcy-36(db66)* X; *kyEx2087* [*gcy-36::gcy-36 odr-1::DsRed2*], **CX9624** *gcy-36(db66)* X; *kyEx2090* [*flp-8::gcy-36 odr-1::DsRed2*], **CX9623** *gcy-36(db66)* X; *kyEx2089* [*flp-8::gcy-36 odr-1::DsRed2*], **CX10293** *kyEx2416* [*flp-17::ChR2::mCherry unc-122::gfp*], **CX10208** *kyEx2366* [*flp-17::G-CaMP2.0 flp-17::mCherry unc-122::gfp*], **CX10212** *gcy-31(ok296)* X; *kyEx2366* [*flp-17::G-CaMP2.0 flp-17::mCherry unc-122::gfp*], **CX10209** *gcy-33(ok232)* V; *kyEx2366* [*flp-17::G-CaMP2.0 flp-17::mCherry unc-122::gfp*], **CX7376** *kyIs511* V [*gcy-36::GCaMP unc-122::gfp*], **CX10945** *gcy-33(ok232)* V; *kyIs511* V [*gcy-36::GCaMP unc-122::gfp*], **CX7984** *gcy-35(ok769)* I; *kyIs511* V [*gcy-36::GCaMP unc-122::gfp*], **CX9796** *kyIs511* V [*gcy-36::GCaMP unc-122::gfp*]; *gcy-36(db66)* X, **CX10583** *gcy-35(ok769)* I; *gcy-31(ok296)* X; *kyEx2366* [*flp-17::G-CaMP2.0 flp-17::mCherry unc-122::gfp*] *kyEx2435* [*flp-17::gcy35 flp-17::gcy-36 odr-1::dsRed2*], **CX10643** *gcy-35(ok769)* I; *gcy-33(ok232)* V; *gcy-31(ok296)* X; *kyEx2366* [*flp-17::G-CaMP2.0 flp-17::mCherry unc-122::gfp*] *kyEx2435* [*flp-17::gcy35 flp-17::gcy-36 odr-1::dsRed2*], **CX10244** *gcy-35(ok769)* I; *gcy-31(ok296)* X; *kyEx2435* [*flp-17::gcy35 flp-17::gcy-36 odr-1::dsRed2*], **CX10368** *gcy-35(ok769)* I; *gcy-31(ok296)* X; *kyEx2478* [*flp-17::gcy35 flp-17::gcy-36 odr-1::dsRed2*], **CX10782** *gcy-35(ok769)* I; *gcy-33(ok232)* V; *gcy-31(ok296)* X; *kyEx2366* [*flp-17::G-CaMP2.0 flp-17::mCherry unc-122::gfp*] *kyEx2478* [*flp-17::gcy35 flp-17::gcy-36 odr-1::dsRed2*]. Germline transformations were carried out as described (Mello et al., 1991).

2. Molecular analysis of *gcy-31* and *gcy-33*

gcy-31(ok296) and *gcy-33(ok232)* mutants were obtained from the *C. elegans* knockout consortium and confirmed via PCR and sequencing from mutant animals. *gcy-31(ok296)* contains a 2505 bp deletion. Breakpoints are 6562 and 9069 with respect to cosmid T07D1. The sequence surrounding the deletion is: GGAAAAAAAACCTTCGCG / TTTGGCTAGTCGTAT. This deletion overlaps the heme binding (H-NOX) domain, and is predicted to result in an out-of-frame splice in the isoforms *gcy-31a* and *gcy-31b*, preventing translation of the catalytic domain. In the isoform *gcy-31c*, the deletion is predicted to result in an in-frame removal of 95 amino acids starting in the heme binding

domain. Thus, mutant worms may retain some *gcy-31c* activity. *gcy-33(ok232)* contains a 1237 bp deletion. Breakpoints are 743 and 1980 with respect to cosmid F57F5. The sequence surrounding the break point is: TGAGAAGTTTATAAAAAAGTA / AA ACTTAAGAGTTTTTCAGTCA. This in-frame deletion replaces the coding sequence of 420 amino acids with one threonine and overlaps with the predicted catalytic domain.

3. Plasmids for expression studies and transgenic rescue

For *gcy-31* gene expression studies, a 12 kb PCR fragment with 4.7 kb of upstream sequence, extending to the predicted *gcy-31* stop codon, was subcloned into a vector (pSM1-SL2-GFP) with the SL2 trans-splice recognition sequence and GFP immediately following the cDNA. The primers used introduced FseI and XbaI sites: 5'-gctctagatcaagttatagattttcgaggagt-3', 5'-ttggccggccttttctacttatgcacgtggt-3'.

For *gcy-33* expression studies, a 14.6 kb PCR fragment with 4.1 kb of upstream sequence, extending to the predicted *gcy-33* stop codon, was subcloned into pSM1-SL2-GFP. The primers used introduced FseI and KpnI sites: 5'-ttggccggccaatagcaattttcgatcagg-3', 5'-cgggggtaccgagctacataataactgcaaac-3'.

For *gcy-31* rescue experiments, the genomic construct described above was injected at 7 ng/ μ l into *gcy-31(ok296)* mutants. All three transgenic lines tested rescued slowing after O₂ downshift. The fosmid WRM0630cF03 was injected at 0.5 ng/ μ l into *gcy-31(ok296)* mutants. Three out of six transgenic lines were rescued for slowing after O₂ downshift. Genomic sequences were used instead of cDNAs because *gcy-31* encodes at least three different proteins from alternatively-spliced mRNAs.

For *gcy-33* rescue experiments, a 3.7 kb *gcy-31* promoter PCR product with FseI and AscI sites and a *gcy-33* cDNA with NheI and KpnI sites were placed into pSM1-SL2-GFP. Expression was observed only in BAG. The construct was injected at 1-25 ng/ μ l into *gcy-33(ok232)* mutants. Five out of nine transgenic lines were rescued for slowing after O₂ downshift. The genomic *gcy-33* expression construct described above was

injected at 5 or 25 ng/μl into *gcy-33(ok232)* mutants. Five out of ten transgenic lines were rescued for slowing after O₂ downshift. None of the ten lines was rescued for slowing after O₂ upshift. A *gcy-33* cDNA under the control of the *gcy-36* promoter (see below) was injected at 15 ng/μl into *gcy-33(ok232)* mutants. None of the four lines was rescued for slowing after O₂ upshift. A *gcy-33* cDNA under the control of the *flp-8* promoter (see below) was injected at 0.5-20 ng/μl into *gcy-33(ok232)* mutants. None of 19 transgenic lines was rescued for slowing after O₂ upshift. The failure to rescue this behavior could result from a requirement for a precise level of *gcy-33* expression, a requirement for distal promoter elements, or a dominant interfering effect of the *gcy-33(ok232)* mutation. Alternatively, the O₂ upshift defect could be caused by a second linked mutation in the *gcy-33(ok232)* strain.

For *gcy-35* rescue experiments and misexpression studies, a 3.5 kb *gcy-35* promoter PCR fragment, a 3.2 kb *flp-8* promoter PCR fragment and a 3.3 kb *flp-17* promoter PCR fragment with FseI and AscI sites were subcloned into a pSM vector with a *gcy-35* cDNA (Chang et al., 2006). The reported expression patterns of these promoter fragments (Cheung et al., 2004; Gray et al., 2004; Kim and Li, 2004) were confirmed by transgenic GFP or mCherry expression (data not shown). *gcy-35::gcy-35* was injected at 0.5 or 20 ng/μl into *gcy-35(ok769)* mutants. All nine transgenic lines were rescued for slowing after O₂ upshift. *flp-8::gcy-35* was injected at 5 or 20 ng/μl into *gcy-35(ok769)* mutants. All five transgenic lines were rescued for slowing after O₂ upshift.

For *gcy-36* rescue experiments and misexpression studies, the *gcy-36* cDNA was inserted into pSM between Sall and KpnI sites and a 1 kb *gcy-36* promoter fragment or the *flp-8* and *flp-17* promoter fragments described above were subcloned into the pSM vector between FseI and AscI. *gcy-36::gcy-36* was injected at 0.5 ng/μl into *gcy-36(db66)* mutants. All three transgenic lines were rescued for slowing after O₂ upshift. *flp-8::gcy-36* was injected at 5 ng/μl. Two transgenic lines were rescued for slowing after O₂ upshift.

flp-17::gcy-35 and *flp-17::gcy-36* were injected at 5 ng/μl each into *gcy-31(ok296) gcy-35(ok769)* double mutants. Five out of seven transgenic lines showed slowing in response to O₂ upshift. The two lines shown in Figure 8 were crossed to CX10208 animals that express GCaMP2.0 in BAG, and to *gcy-33(ok232)* mutants. Control experiments in Figure 7 and Figure 8 were carried out in non-transgenic siblings from the same clonal lines.

The channelrhodopsin2 (ChR2) cDNA was isolated by RT-PCR from *Chlamydomonas reinhardtii* total RNA using the oligonucleotides 5'-gcgcatgatcggctagcatggattatggaggcggccc-3' and 5'-cgcgatccgatggtaccctcttgccgggtgccctgttg-3', and cloned into the vector pSMmCherry at the NheI and KpnI sites to generate an mCherry fusion protein. The higher conductance mutation H134R17 was inserted via QuikChange (Stratagene). The *flp-17* promoter was inserted at FseI and AscI as above. The construct was injected at 1.5 ng/μl. Two transgenic lines showed light-induced slowing responses.

Oligonucleotides used to amplify promoter constructs:

Pgcy-31:

5'-tgatggccggccatgtcatatctaaagatgc-3', 5'-taagggcgcgcccggcgggtgaaaattgaaaatg-3'

Pgcy-35:

5'-ttggccggccttatggcggttgaaacct-3', 5'-ttggcgcgccaatattctactctccgcaa-3'

Pflp-8:

5'-aaaaggccggcccttcgtgatggagttcgcagcaatgag-3',

5'-aaaaggcgcgcccattttctacttgaaaagtgtggactgagcactgctc-3'

Pflp-17:

5'-ttggccggccccttgaagcttttctctg-3', 5'-ttggcgcgccccttgaaaaataaagttttgcg-3'

Pgcy-36:

5'-ttggccggccatgatgttgtagatggggtttg-3', 5'-ttggcgcgcccctgttggttagcccttgttgaattt-3'.

4. Supplementary references

- Boon, E. M., and Marletta, M. A. (2005). Ligand discrimination in soluble guanylate cyclase and the H-NOX family of heme sensor proteins. *Curr Opin Chem Biol* 9, 441-446.
- Brenner, S. (1974). The genetics of *Caenorhabditis elegans*. *Genetics* 77, 71-94.
- Chang, A.J., Chronis, N., Karow, D.S., Marletta, M.A., and Bargmann, C.I. (2006). A Distributed Chemosensory Circuit for Oxygen Preference in *C. elegans*. *PLoS Biol.* 4, e274.
- Cheung, B. H., Arellano-Carbajal, F., Rybicki, I., and de Bono, M. (2004). Soluble guanylate cyclases act in neurons exposed to the body fluid to promote *C. elegans* aggregation behavior. *Curr Biol* 14, 1105-1111.
- Gray, J. M., Karow, D. S., Lu, H., Chang, A. J., Chang, J. S., Ellis, R. E., Marletta, M. A., and Bargmann, C. I. (2004). Oxygen sensation and social feeding mediated by a *C. elegans* guanylate cyclase homologue. *Nature* 430, 317-322.
- Kim, K., and Li, C. (2004). Expression and regulation of an FMRFamide-related neuropeptide gene family in *Caenorhabditis elegans*. *J Comp Neurol* 475, 540-550.
- Mello, C. C., Kramer, J. M., Stinchcomb, D., and Ambros, V. (1991). Efficient gene transfer in *C. elegans*: extrachromosomal maintenance and integration of transforming sequences. *Embo J* 10, 3959-3970.

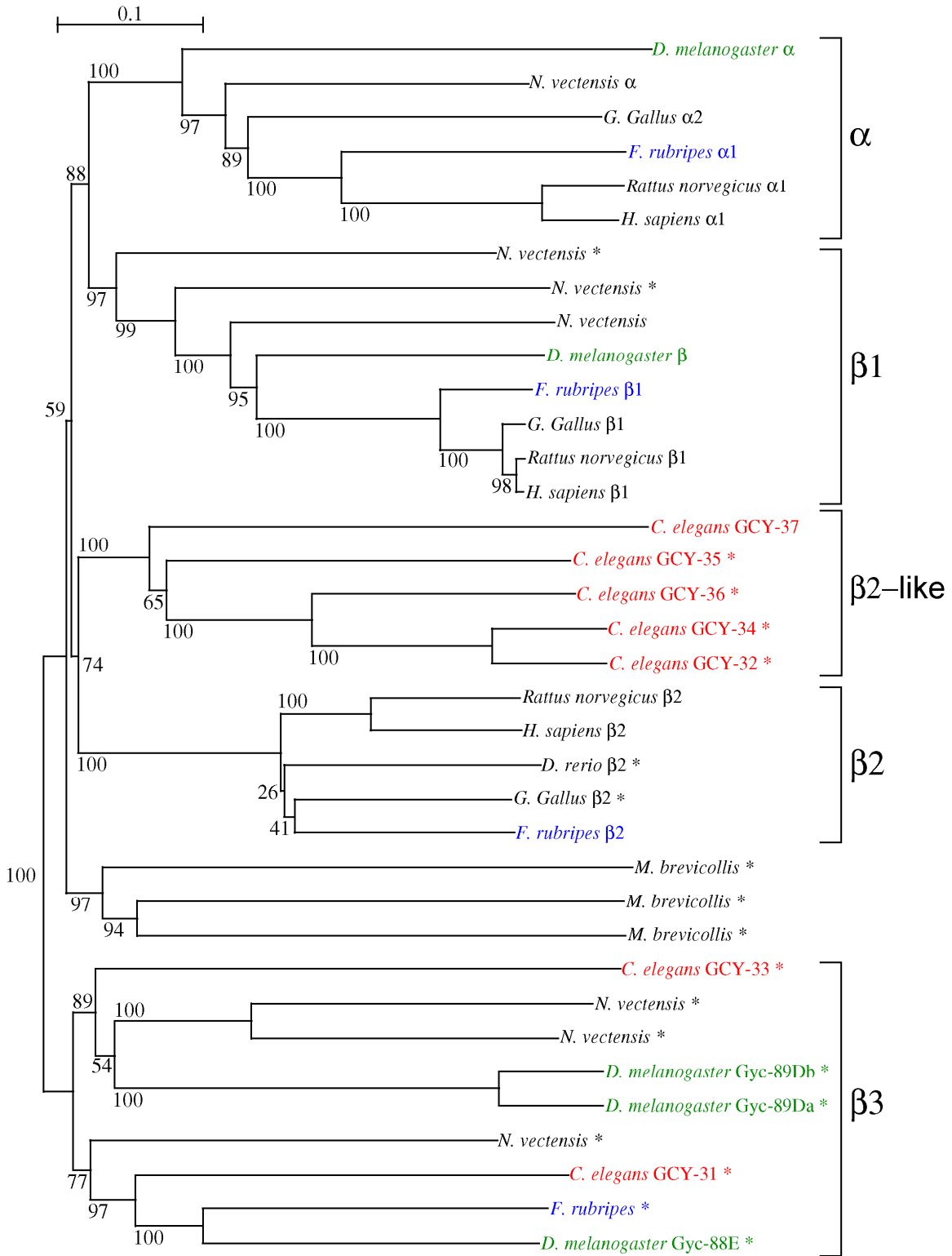
5. Supplementary table

Bonferroni's Multiple Comparison Test (Figure 3)

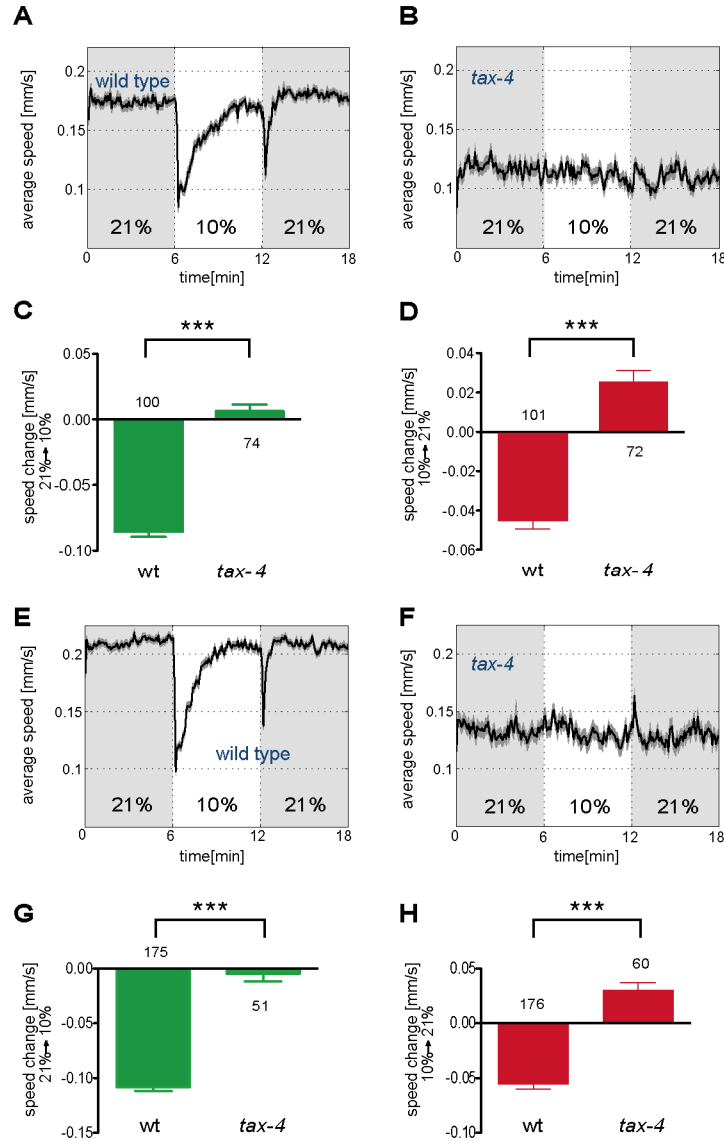
| URX | |
|-------------------|-----------------------|
| comparison | <i>P</i> value |
| 4-10% vs 4-15% | 0.001-0.01 |
| 4-10% vs 4-21% | <0.001 |
| 4-10% vs 10-15% | >0.05 |
| 4-10% vs 10-21% | <0.001 |
| 4-10% vs 15-21% | <0.001 |
| 4-15% vs 4-21% | <0.001 |
| 4-15% vs 10-15% | >0.05 |
| 4-15% vs 10-21% | >0.05 |
| 4-15% vs 15-21% | >0.05 |
| 4-21% vs 10-15% | <0.001 |
| 4-21% vs 10-21% | <0.001 |
| 4-21% vs 15-21% | <0.001 |
| 10-15% vs 10-21% | 0.01-0.05 |
| 10-15% vs 15-21% | 0.001-0.01 |
| 10-21% vs 15-21% | >0.05 |

| BAG | |
|-------------------|-----------------------|
| comparison | <i>P</i> value |
| 21-15% vs 21-10% | >0.05 |
| 21-15% vs 21-4% | <0.001 |
| 21-15% vs 15-10% | >0.05 |
| 21-15% vs 15-4% | <0.001 |
| 21-15% vs 10-4% | 0.001-0.01 |
| 21-10% vs 21-4% | <0.001 |
| 21-10% vs 15-10% | >0.05 |
| 21-10% vs 15-4% | 0.01-0.05 |
| 21-10% vs 10-4% | >0.05 |
| 21-04% vs 15-10% | <0.001 |
| 21-04% vs 15-4% | 0.01-0.05 |
| 21-04% vs 10-4% | 0.001-0.01 |
| 15-10% vs 15-4% | 0.01-0.05 |
| 15-10% vs 10-4% | >0.05 |
| 15-04% vs 10-4% | >0.05 |

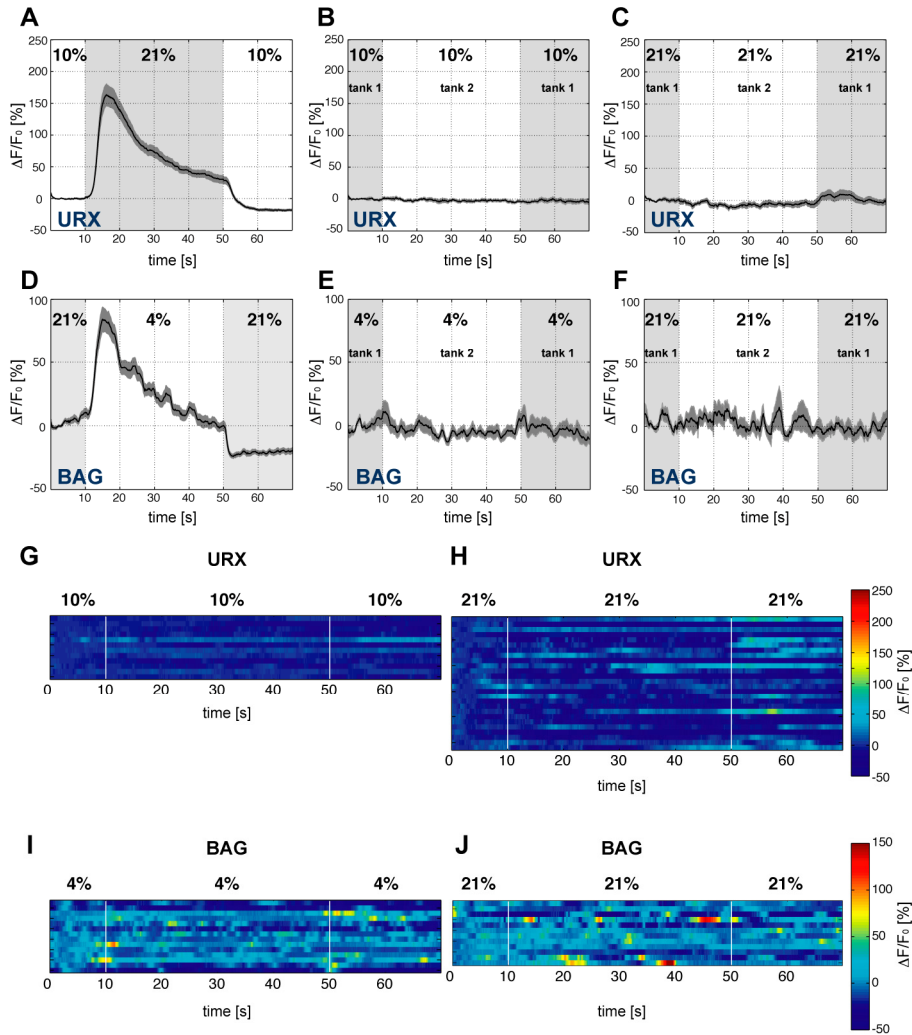
6. Supplementary figures and legends



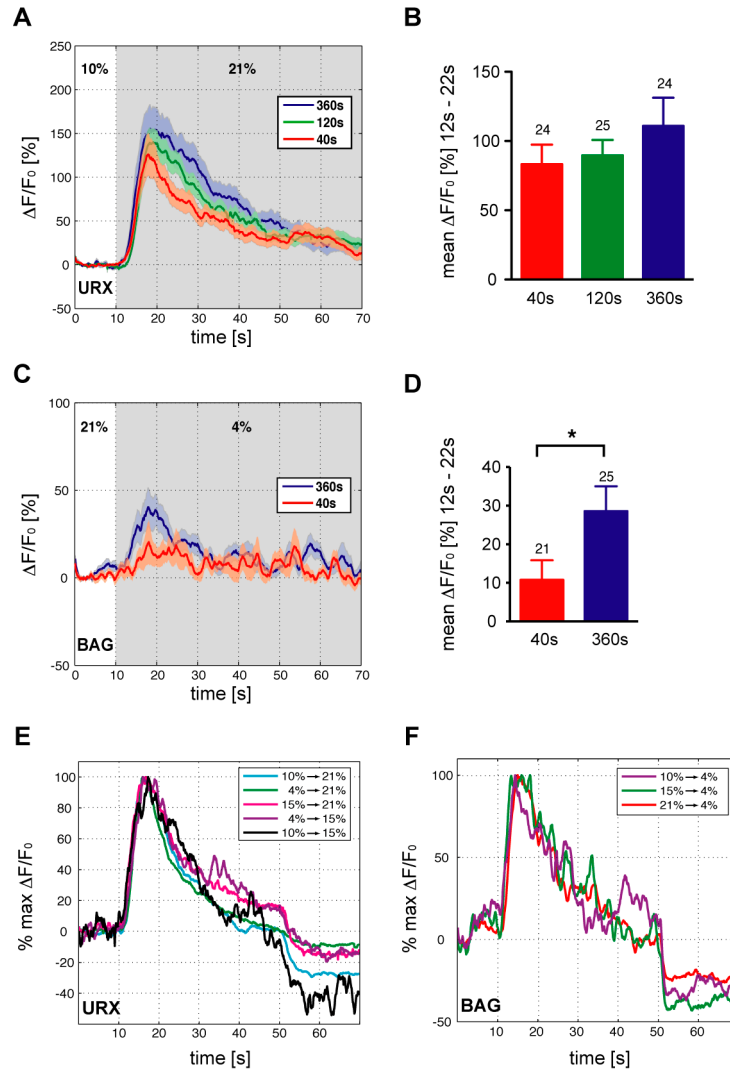
Supplementary Figure 1. Phylogeny of soluble guanylate cyclases. Phylogenetic tree derived from an amino acid alignment using ClustalX (2.0) software. Numbers indicate bootstrap support. Scale bar indicates genetic distance. Asterisks show sGCs that bear a tyrosine residue in the heme binding pocket suggesting the ability to bind oxygen (Boon and Marletta, 2005). Accession numbers of protein sequences from top to bottom: *D. melanogaster* α (swissprot Q07093); *N. vectensis* α (sptrembl A7RN71); *G. gallus* $\alpha 2$ (UniParc UPI0000E7FC09); *F. rubripes* $\alpha 1$ (sptrembl Q90VV5); *R. norvegicus* $\alpha 1$ (UniProtKB Q5U330); *H. sapiens* $\alpha 1$ (UniProtKB Q02108.2); *N. vectensis* (sptrembl A7RN72); *N. vectensis* (sptrembl A7RN70); *N. vectensis* (sptrembl A7RN69); *D. melanogaster* β (sptrembl Q24086); *F. rubripes* $\beta 1$ (sptrembl Q90VY5); *G. gallus* $\beta 1$ (UniParc UPI0000610CA4); *H. sapiens* $\beta 1$ (swissprot Q02153); *R. norvegicus* $\beta 1$ (swissprot P20595); *C. elegans* GCY-37 (UniProtKB Q6DNF3); *C. elegans* GCY-35 (UniProtKB O02298); *C. elegans* GCY-36 (UniProtKB Q6DNF4); *C. elegans* GCY-34 (UniProtKB P92006); *C. elegans* GCY-32 (UniProtKB Q6DNF7); *R. norvegicus* $\beta 2$ (swissprot P22717); *H. sapiens* $\beta 2$ (swissprot O75343); *D. rerio* $\beta 2$ (UniParc UPI000175FF10); *G. gallus* $\beta 2$ (UniParc UPI0000ECB130); *F. rubripes* $\beta 2$ (Ensembl SINFRUT00000135798.3); *M. brevicollis* (sptrembl A9UU55); *M. brevicollis* (sptrembl A9UZU0); *M. brevicollis* (sptrembl A9V7H3); *C. elegans* GCY-33 (UniProtKB P90895); *N. vectensis* (sptrembl A7S7B3); *N. vectensis* (sptrembl A7S7B2); *D. melanogaster* Gyc-89Db (UniProtKB Q9VEU5); *D. melanogaster* Gyc-89Da (UniProtKB Q9VEU6); *N. vectensis* (sptrembl A7RZH8); *C. elegans* GCY-31 (UniProtKB Q86C56); *F. rubripes* (Ensembl SINFRUT00000152493.3); *D. melanogaster* Gyc-88E (UniProtKB Q8INF0).



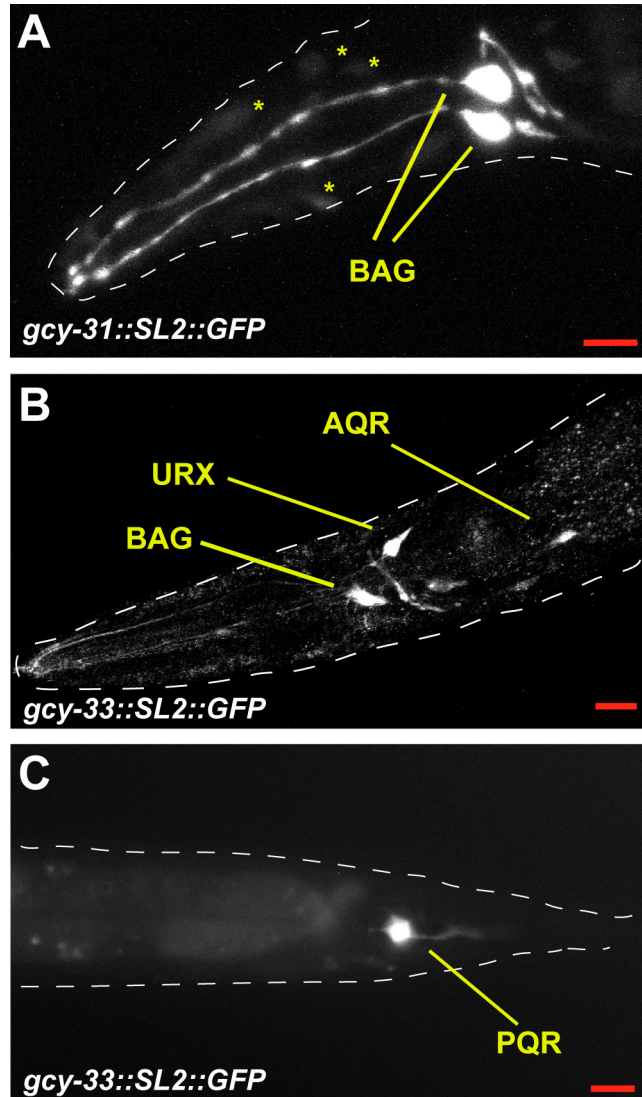
Supplementary Figure 2. The cGMP gated cation channel TAX-4 is required for O₂-regulated slowing. (A,B,E,F) Locomotion speed off food. Traces show average speed and dark shading indicates standard error of the mean (SEM). Light shading marks intervals at 21% O₂. *tax-4* mutants have a significantly slower basal locomotion speed than wild-type, and do not respond to O₂ changes regardless of basal speed; two sets of experiments with different basal locomotion speeds are shown. **(A,E)** Wild-type animals. Average basal speed: (A) 0.18 ± 0.01 (SD) mm/s (range 0.16-0.19), n=9 assays (E) 0.21 ± 0.02 mm/s (range 0.18-0.24), n=15 assays. **(B,F)** *tax-4(ks28)* mutants tested at similar times to controls in (A) and (E), respectively. Average basal speed: (B) 0.12 ± 0.01 mm/s (range 0.10-0.14), n=6 assays (F) 0.14 ± 0.01 mm/s (range 0.12-0.15), n=6 assays. **(C,D,G,H)** Average speed changes (difference of the means of 10 second intervals before and after the switch) of animals with indicated genotypes. Error bars indicate SEM. Asterisks indicate significance by t-test (***) $P < 0.0001$). The numbers of animal tracks analyzed are indicated. **(C,G)** Response to O₂ downshift. **(D,H)** Response to O₂ upshift.



Supplementary Figure 3. Control calcium traces for URX and BAG neurons. (A-F) Measurements of neural activity by calcium imaging of URX and BAG neurons. Black traces show the average percent change of G-CaMP fluorescence ($\Delta F/F_0$) and dark shading shows standard error of the mean (SEM). Light shading marks intervals with different gas sources. **(A)** URX activity as in Figure 2D. **(B)** URX activity while switching between two tanks containing 10% O₂. **(C)** URX activity while switching between two tanks containing 21% O₂. **(D)** BAG activity as in Figure 2H. **(E)** BAG activity while switching between two tanks containing 4% O₂. **(F)** BAG activity while switching between two tanks containing 21% O₂. **(G,H)** Individual control URX responses in 10% O₂ (**G**, n=12) and in 21% O₂ (**H**, n=26) (same datasets as in B,C). **(I,J)** Individual control BAG responses in 4% O₂ (**I**, n=14) and in 21% O₂ (**J**, n=12) (same datasets as in E,F). For **(G-J)** each row represents one recording.



Supplementary Figure 4. Kinetics of calcium responses in URX and BAG. (A-D) Calcium imaging of URX and BAG neurons after different pre-incubation times at start concentrations. **(A,B)** URX. Animals were held at 10% O₂ for the indicated times before switching to 21% O₂. Recordings started at the last 10 seconds at 10% O₂. **(C,D)** BAG. After a 6 min holding time at 4% O₂, animals were held at 21% O₂ for the indicated times before switching back to 4% O₂. Recordings started at the last 10 seconds at 21% O₂. (A) and (C) show the average percent change of G-CaMP fluorescence ($\Delta F/F_0$); shading shows standard error of the mean (SEM). (B) and (D) show average $\Delta F/F_0$ from 12s-22s; error bars indicate SEM. Asterisk indicates significance by t-test, $P = 0.04$. The numbers of recordings analyzed are indicated. **(E)** A subset of traces shown in Figure 3A normalized to 100% maximum response. **(F)** A subset of traces shown in Figure 3D normalized to 100% maximum response.



Supplementary Figure 5. Expression of *gcy-31* and *gcy-33* reporter genes. Confocal (A,B) and epifluorescence (C) images of green fluorescent protein (GFP) expressed in sensory neurons. (A) Head of an animal expressing a genomic *gcy-31* clone with 4.7 kb of upstream region, in a bicistronic mRNA with GFP. Identified neurons are indicated. Asterisks in (A) mark additional head cells that express GFP faintly; the gut also expresses GFP. (B,C) Head and tail of a transgenic animal expressing a genomic *gcy-33* clone with 4.1 kb of upstream region, in a bicistronic mRNA with GFP. Scale bars represent 10 μm .